SUPPORTING INFORMATION

Lipid A structural determination from a single colony

Hyojik Yang[1], Richard D. Smith[1, 2], Courtney E. Chandler[1], J. Kristie Johnson[2], Shelley N. Jackson[3], Amina S. Woods[4,5], Alison J. Scott[1, 6], David R. Goodlett[*7, 8], and Robert K. Ernst[*1]

[1] Department of Microbial Pathogenesis, School of Dentistry, University of Maryland, Baltimore, MD 21201 USA

[2] Department of Pathology, School of Medicine, University of Maryland, Baltimore, MD 21201 USA

[3] Translational Analytical Core, NIDA IRP, NIH, Biomedical Research Center, 251 Bayview Boulevard, Suite 200, Room 01B216, Baltimore, MD 21224, USA

[4] Structural Biology Core, NIDA IRP, NIH, 333 Cassell Drive, Room 1120, Baltimore, MD 21224, USA

[5] Pharmacology and Molecular Sciences, Johns Hopkins University School of Medicine. Baltimore, MD 21205 USA

[6] Maastricht MultiModal Molecular Imaging (M4I) Institute, Maastricht University, Maastricht 6229 ER, Netherlands

[7] Department of Biochemistry and Microbiology, University of Victoria, 3800 Finnerty Road. Victoria, BC V8P 5C2, Canada

[8] International Centre for Cancer Vaccine Science, University of Gdańsk, ul. Kładki 24 80-822 Gdańsk, Poland

* Corresponding

Robert K. Ernst : rkernst@umaryland.edu

David R. Goodlett : goodlett@uvic.ca

KEYWORDS : Lipid A, Gram-negative bacteria, Tandem Mass Spectrometry, FLAT^n, Structural analysis

SUPPORTING INFORMATION

EXPERIMENTAL SECTION

Materials

Methanol (MeOH, 98%), Norharmane (NRM, 98%)[1,2], and chloroform (HPLC grade) were purchased from Sigma Aldrich (St. Louis, MO, USA). Certified endotoxin-free water was sourced from Gibco (Grand Island, NY, USA). ITO glass slides were obtained from Delta Technologies LTD (Loveland, CO, USA). All other chemicals were obtained from Sigma Aldrich, unless otherwise noted.

Bacteria Strains and Cultivation

Bacterial strains used included *Escherichia coli* ATCC 25922 (*E. coli, Ec*) and *Pseudomonas aeruginosa* ATCC 31482 (*P. aeruginosa, Pa*). The following strains expressing the *mcr-1* gene, a phosphoethanolamine transferase *in trans* were also used: *Escherichia coli* ATCC 25922 (*mcr-1 E. coli*), *Klebsiella pneumoniae* ATCC 13883 (*mcr-1 K. pneumoniae, Kp*), *Acinetobacter baumannii* ATCC 17978 (*mcr-1 A. baumannii, Ab*), and *Pseudomonas aeruginosa* ATCC 31482 (*mcr-1 P. aeruginosa*).[3] Individual isolates were initially cultivated on Lysogeny broth (LB, Becton-Dickenson, Hunt Valley, MD, USA) supplemented with 1.5% Bacto-agar. Strains expressing *mcr-1* from plasmids in *mcr-1 E. coli, mcr-1 P. aeruginosa, and mcr-1 A. baumannii* were selected on gentamicin (50 µg/mL). Strains expressing *mcr-1 K. pneumoniae* were selected on chloramphenicol (25 µg/mL).

Mass Spectrometry

A Bruker MALDI (tims TOF) MS and Thermo MALDI Linear Ion Trap (LTQ)-XL-Orbitrap MS (San Jose, CA) were used for FLAT^n experiments. MALDI (tims TOF) MS equipped with a dual ESI/MALDI source with a SmartBeam 3D 10 KHz frequency tripled Nd:YAG laser (355 nm). The system was operated in “qTOF” mode (TIMS deactivated). Ion transfer tuning was used with the following parameters: Funnel 1 RF: 440.0 Vpp, Funnel 2 RF: 490.0 Vpp, Multipole RF 490.0 Vpp, is CID Energy: 0.0 eV, and Deflection Delta: -60.0 V. Quadrupole has been used with the following values for MS mode: Ion Energy: 4.0 eV and Low Mass 700.00 *m/z*. Collision cell activation of ions used the following

values for MS mode. Collision Energy: 9.0 eV and Collision RF :3900.0 Vpp. In the MS/MS mode, the precursor ion was chosen by typing targeted *m/z* value including two digits to the right of the decimal point. Typical isolation width and collision energy were set to 4 - 6 *m/z* and 100 - 110 eV, respectively. Focus Pre TOF used the following values for Transfer Time 110.0 µs and Pre Pulse Storage 9.0 µs. Agilent ESI Tune Mix was used to perform calibration of the *m/z* scale. MALDI parameters in qTOF were optimized to maximize intensity by tuning ion optics, laser intensity, and laser focus. All mass spectra were collected at 104 µm laser diameter with beam scan on using 800 laser shots per spot and 70 and 80% laser power, respectively. Both MS and MS/MS data were collected in negative ion mode. A MALDI-LTQ-XL Orbitrap MS was used as a comparison to MALDI (tims TOF) MS. As expected the qTOF data provided a more useful array of fragment ions for structure interpretation than the ion trap. MS data were acquired in negative ion mode with a mass resolution of 60,000 at *m*/*z* 400. In all cases, 10mg/mL of norharman (NRM)[1,4] in 1:2 MeOH:$CHCl_3$ (v:v) was used for lipid A detection. NRM solution (1 µL) was deposited on the sample spot.

Data Processing

Xcaliber software was used for MALDI LTQ-XL-Orbitrap MS or MS/MS data acquisition and processing. All MALDI (timsTOF) MS and MS/MS data were visualized using mMass (Ver 5.5.0).[5] Peak picking was conducted in mMass. Identification of all fragment ions were determined based on Chemdraw Ultra (Ver10.0) and Bruker Compass DataAnalysis 4.2 SR1.

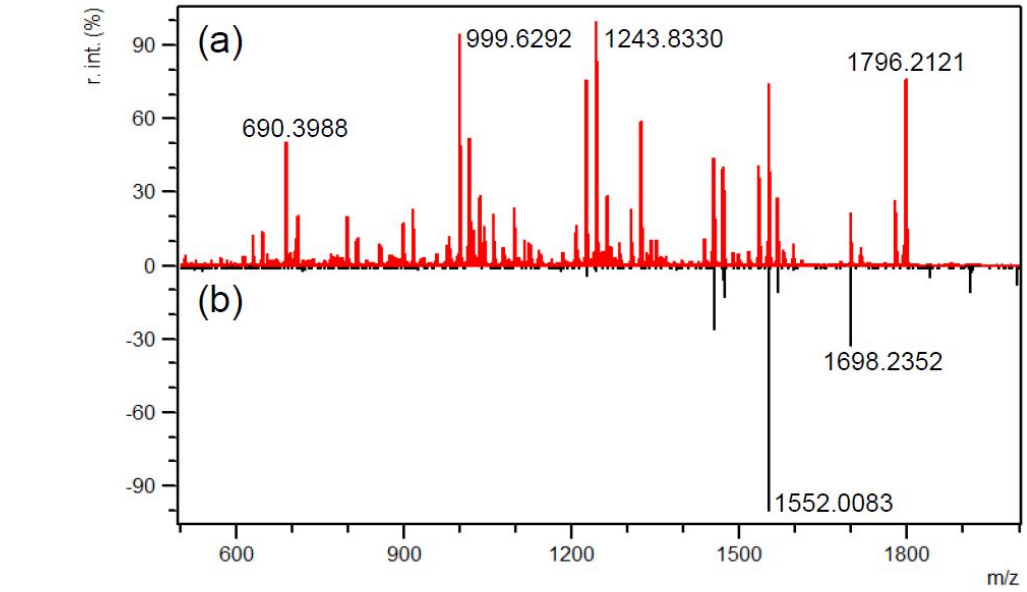

(c)

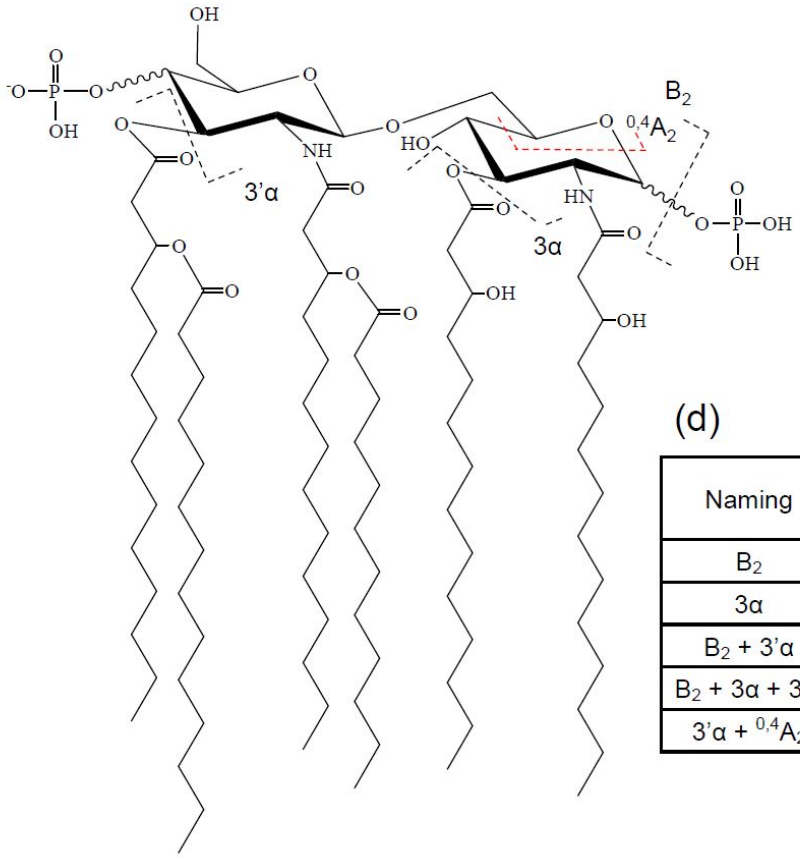

(d)

Naming	*m/z* (theory)	*m/z* (expt)	Error (ppm)
B_2	1698.2352	1698.2241	-6.5
3α	1552.0083	1551.9920	-10.5
B_2 + 3'α	1243.8330	1243.8219	-8.9
B_2 + 3α + 3'α	999.6292	999.6199	-9.3
3'α + $^{0,4}A_2$	690.3988	690.3950	-5.5

Figure S1. FLAT^n tandem mass spectra from precursor ion at *m/z* 1796.2121 using (a) MALDI (Bruker tims TOF) MS and (b) MALDI LTQ-XL-Orbitrap MS. (c) structure of *E. coli* lipid A from FLAT^n, and (d) list of assigned ions.

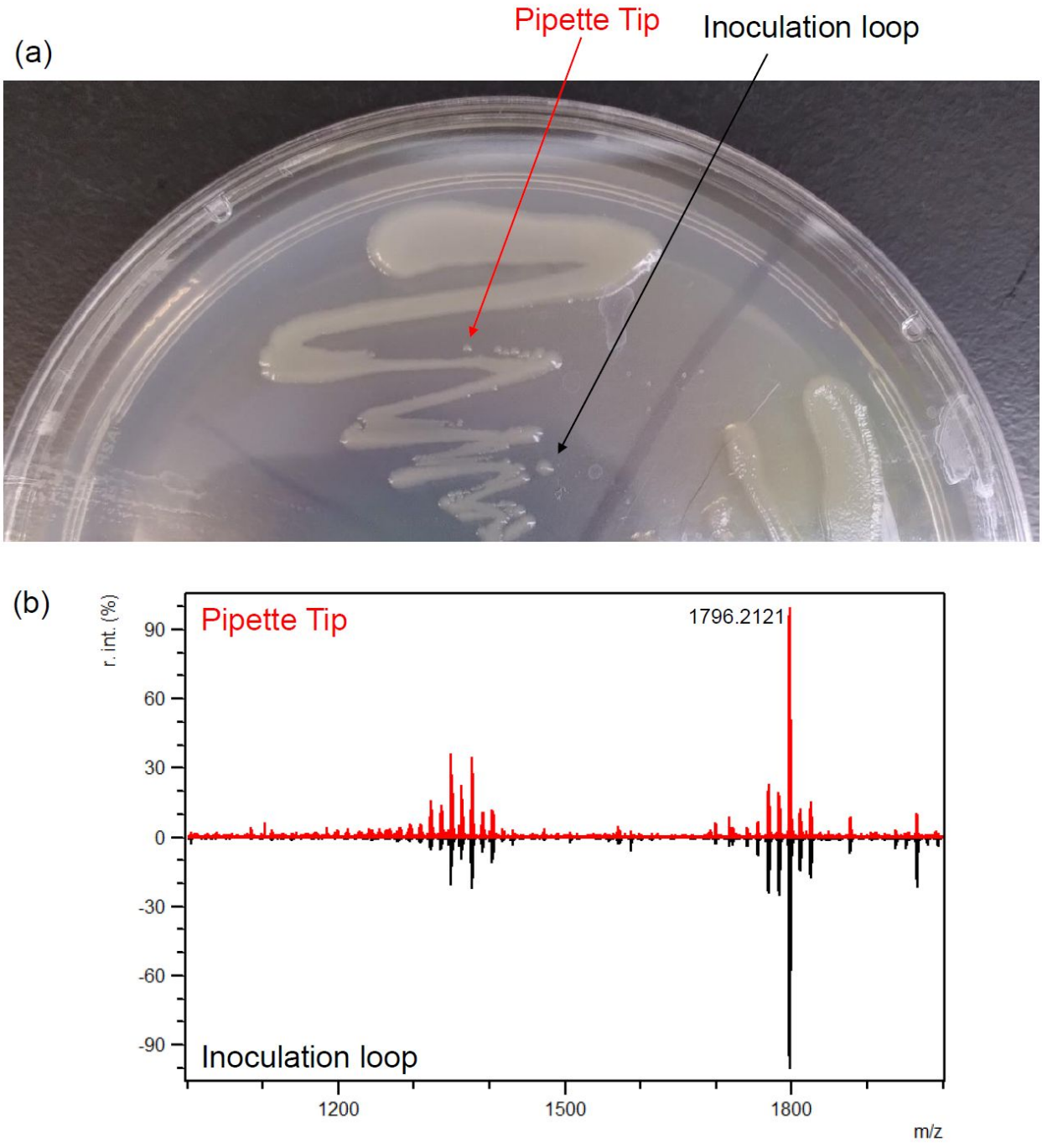

Figure S2. (a) An image of *E. coli* single colonies on agar plate. (b) FLAT mass spectra were obtained from the colony using a pipette tip (Top) and inoculation loop (bottom). In case of inoculation loop, after picking the colony, the sample was dissolved in deionized water. The detail of the method is in supplementary information. The *m/z* 1796.2121 indicates lipid A ion from *E. coli.*

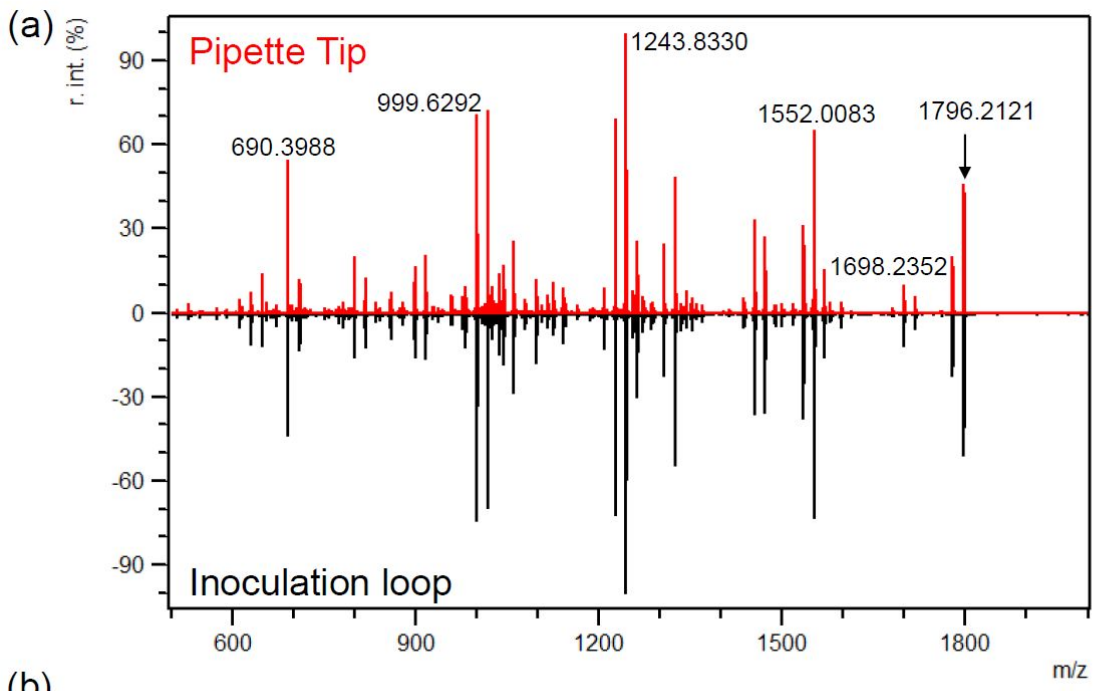

(b)

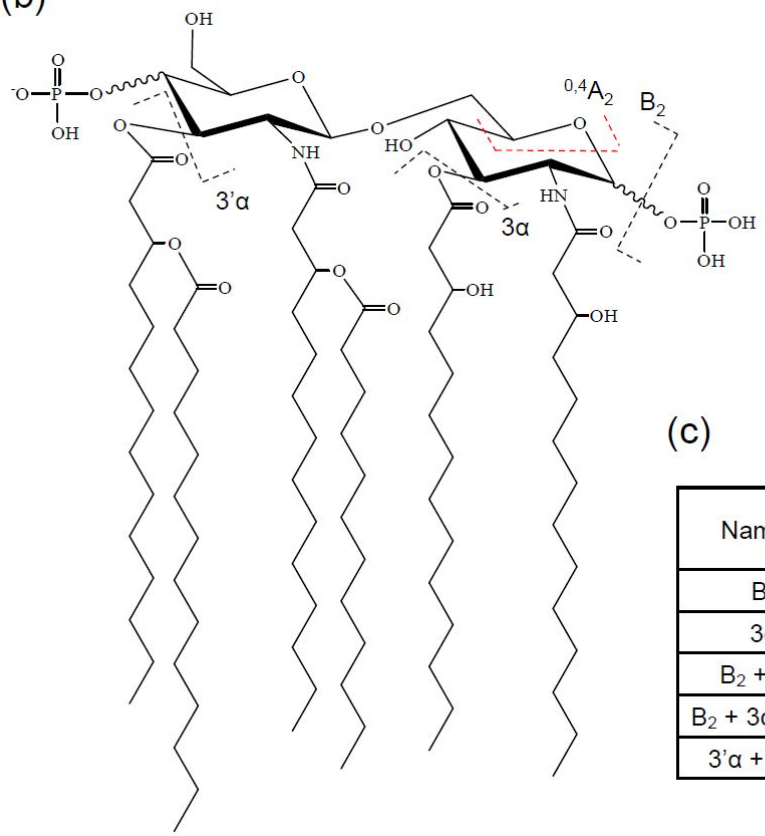

(c)

Naming	*m/z* (theory)	*m/z* (expt)	Error (ppm)
B_2	1698.2352	1698.2003	-20.6
3α	1552.0083	1551.9763	-20.6
B_2 + 3'α	1243.8330	1243.8077	-20.3
B_2 + 3α + 3'α	999.6292	999.6096	-19.6
3'α + $^{0,4}A_2$	690.3988	690.3866	-17.7

Figure S3. (a) FLAT^n mass spectrum from precursor ion at *m/z* 1796.2121 (b) structure of *E. coli* lipid A from FLAT^n, and (c) list of assigned ions.

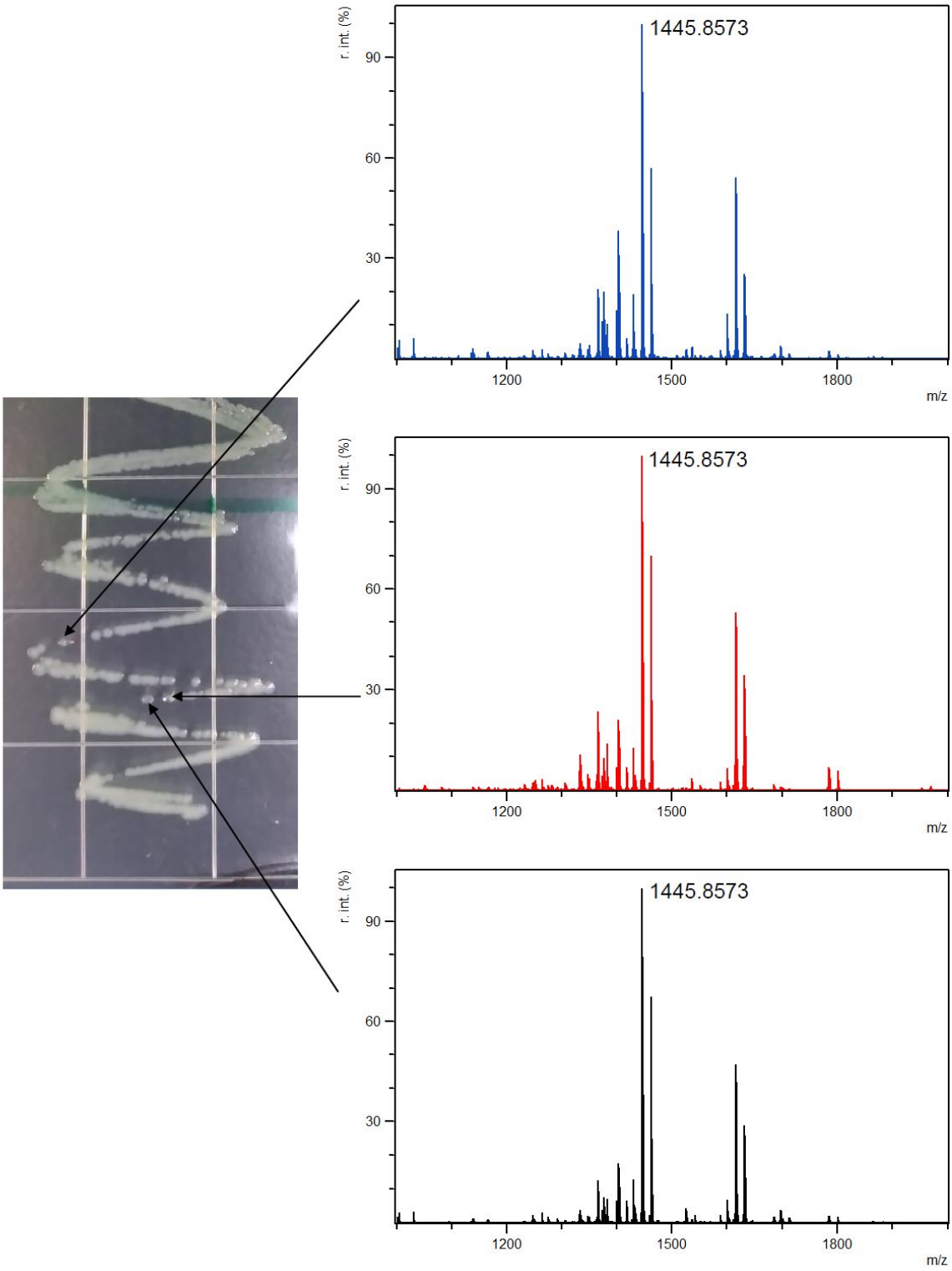

Figure S4. An image of single colonies on agar plate. FLAT^n mass spectra from each colony. The *m/z* 1445.8573 indicates lipid A from the *P. aeruginosa* colony.

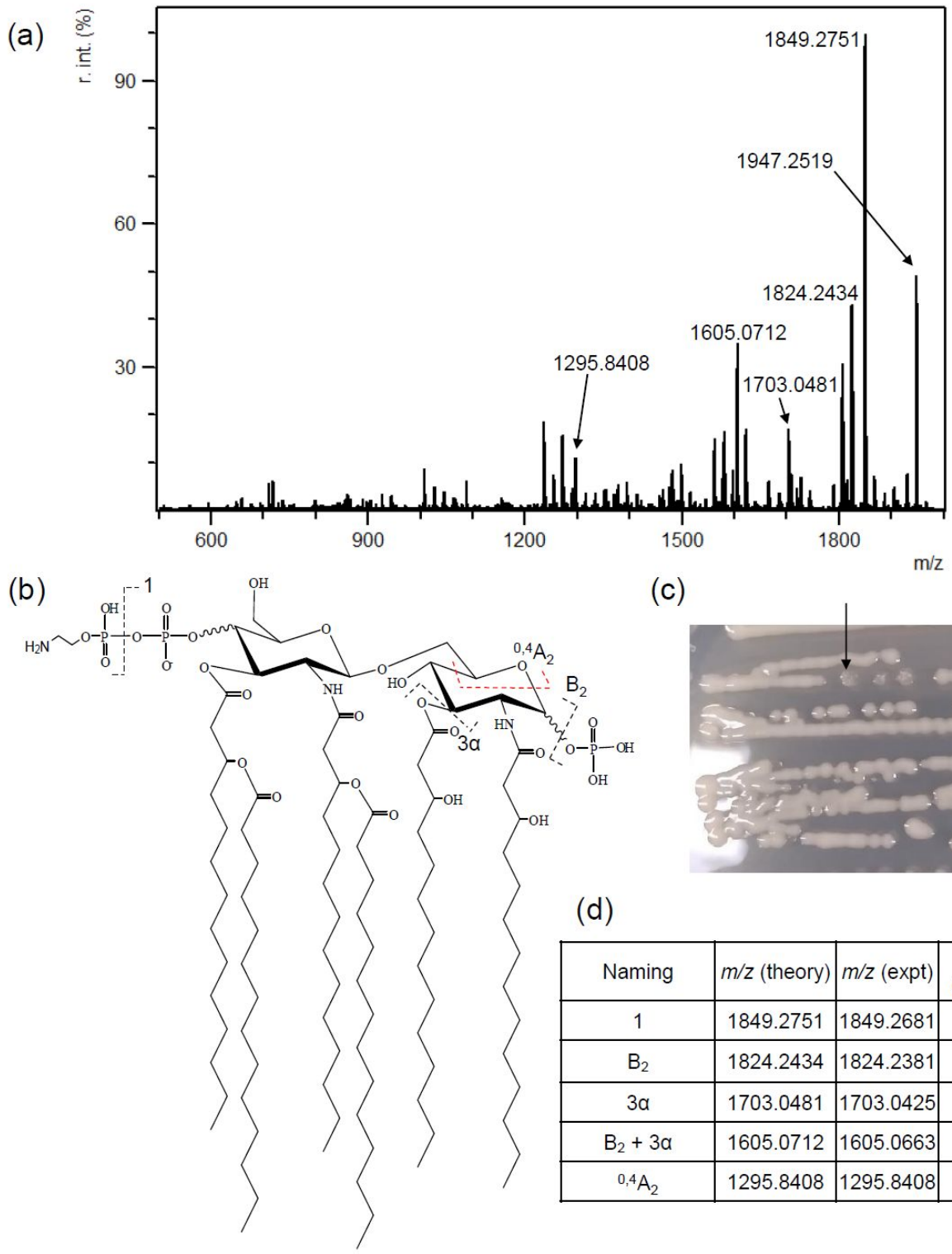

(d)

Naming	*m/z* (theory)	*m/z* (expt)	Error (ppm)
1	1849.2751	1849.2681	-3.8
B_2	1824.2434	1824.2381	-2.9
3α	1703.0481	1703.0425	-3.3
B_2 + 3α	1605.0712	1605.0663	-3.1
$^{0,4}A_2$	1295.8408	1295.8408	0.0

Figure S5. (a) FLAT^n mass spectrum from precursor ion at *m/z* 1947.2519 (b) structure of *K. pneumoniae* expressing *mcr-1* lipid A from FLAT^n (c) An image of single colony of *K. pneumoniae* expressing *mcr-1, and* (d) list of assigned ions.

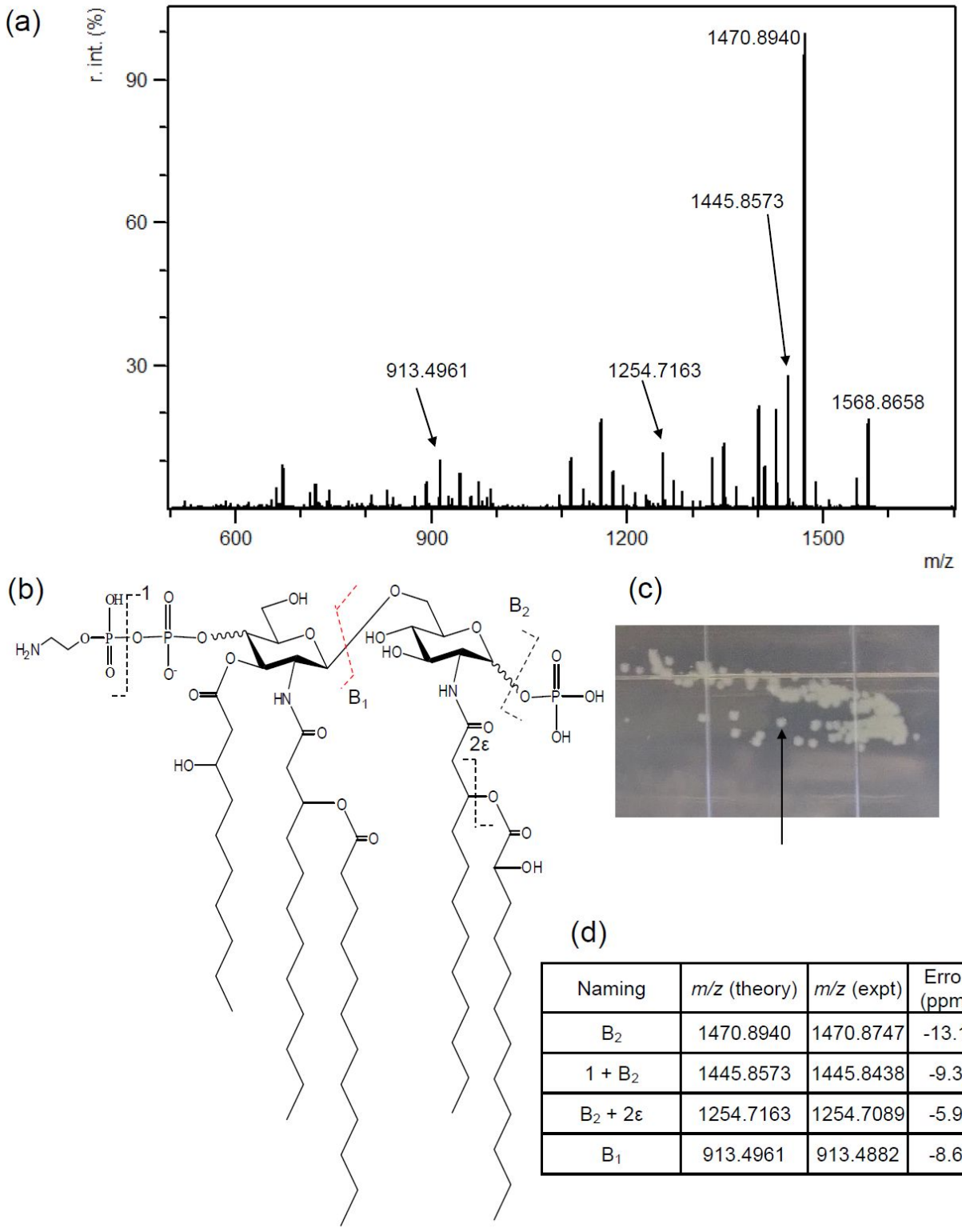

(d)

Naming	*m/z* (theory)	*m/z* (expt)	Error (ppm)
B_2	1470.8940	1470.8747	-13.1
1 + B_2	1445.8573	1445.8438	-9.3
B_2 + 2ε	1254.7163	1254.7089	-5.9
B_1	913.4961	913.4882	-8.6

Figure S6. (a) FLAT^n mass spectrum from precursor ion at *m/z* 1568.8658 (b) structure of *P. aeruginosa* expressing *mcr-1* lipid A from FLAT^n (c) An image of single colony of *P. aeruginosa* expressing *mcr-1*, and (d) list of assigned ions.

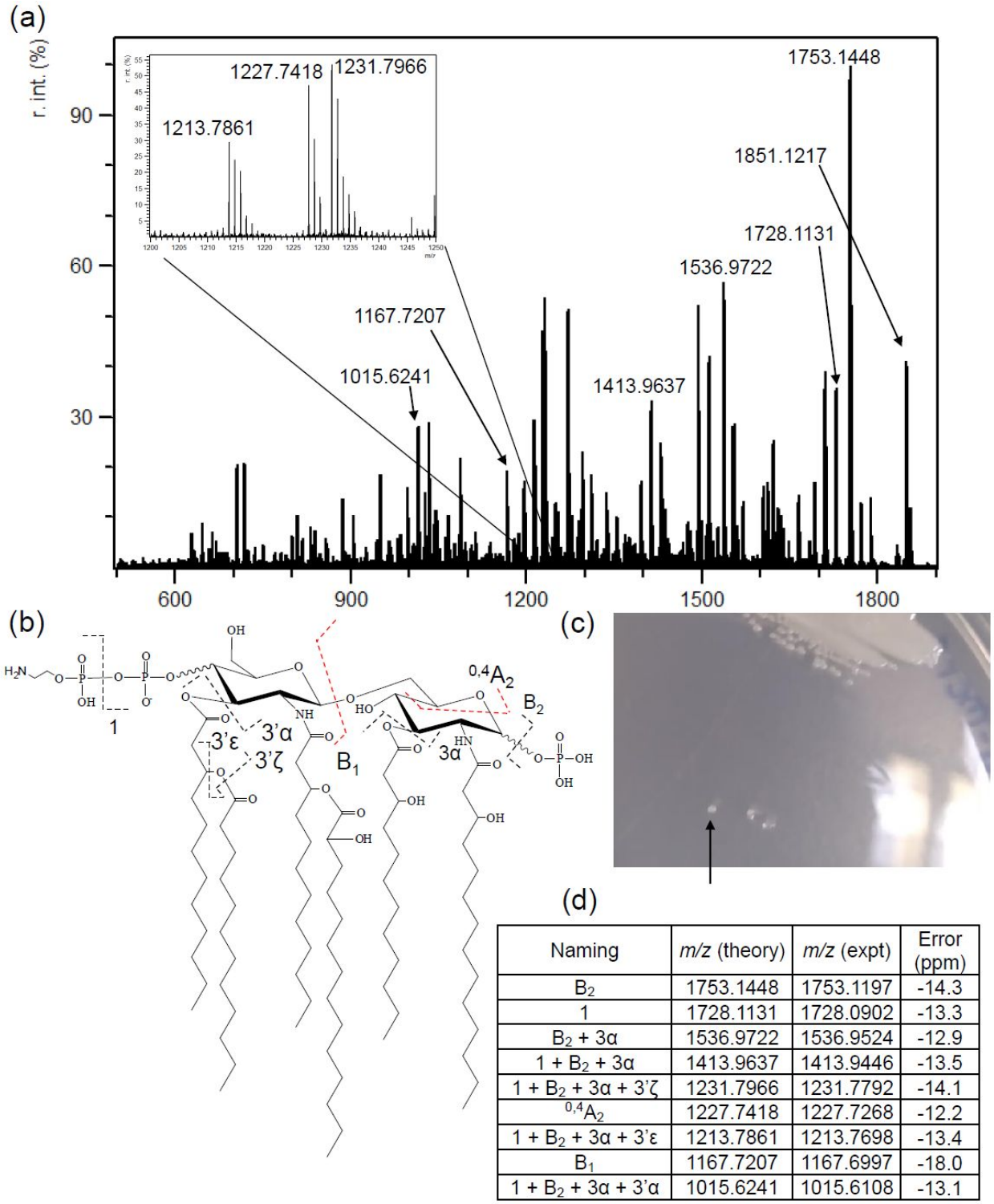

Naming	*m/z* (theory)	*m/z* (expt)	Error (ppm)
B_2	1753.1448	1753.1197	-14.3
1	1728.1131	1728.0902	-13.3
B_2 + 3α	1536.9722	1536.9524	-12.9
1 + B_2 + 3α	1413.9637	1413.9446	-13.5
1 + B_2 + 3α + 3'ζ	1231.7966	1231.7792	-14.1
$^{0,4}A_2$	1227.7418	1227.7268	-12.2
1 + B_2 + 3α + 3'ε	1213.7861	1213.7698	-13.4
B_1	1167.7207	1167.6997	-18.0
1 + B_2 + 3α + 3'α	1015.6241	1015.6108	-13.1

Figure S7. (a) FLAT^n mass spectrum from precursor ion at *m/z* 1851.1217 (b) structure of *A. baumannii* expressing *mcr-1* lipid A from FLAT^n (c) An image of single colony of *A. baumannii* expressing *mcr-1,* and (d) list of assigned ions.

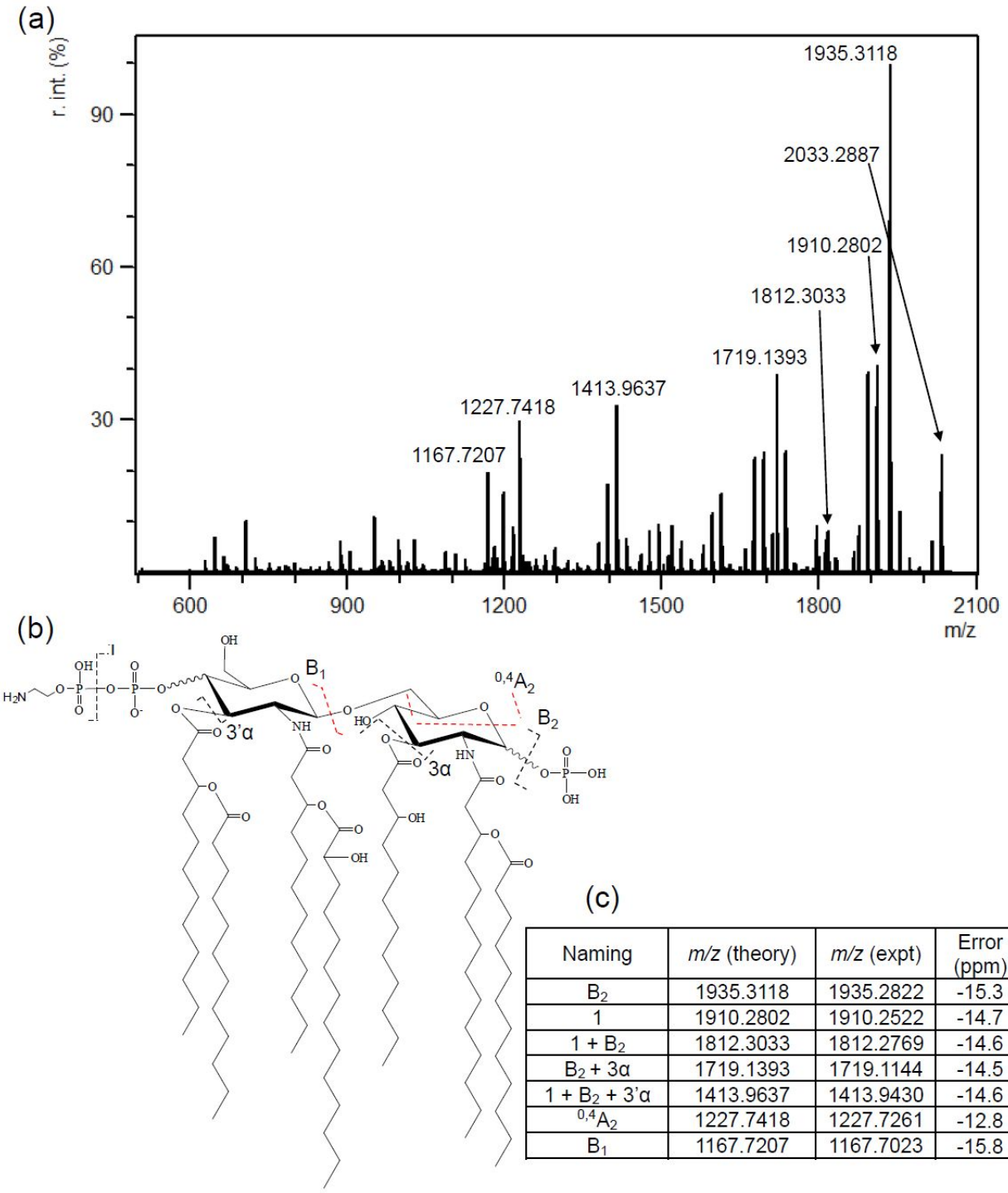

Naming	*m/z* (theory)	*m/z* (expt)	Error (ppm)
B_2	1935.3118	1935.2822	-15.3
1	1910.2802	1910.2522	-14.7
1 + B_2	1812.3033	1812.2769	-14.6
B_2 + 3α	1719.1393	1719.1144	-14.5
1 + B_2 + 3'α	1413.9637	1413.9430	-14.6
$^{0,4}A_2$	1227.7418	1227.7261	-12.8
B_1	1167.7207	1167.7023	-15.8

Figure S8. (a) FLAT^n mass spectrum from precursor ion at *m/z* 2033.2887 (b) structure of *A. baumannii* expressing *mcr-1* lipid A from FLAT^n, and (c) list of assigned ions.

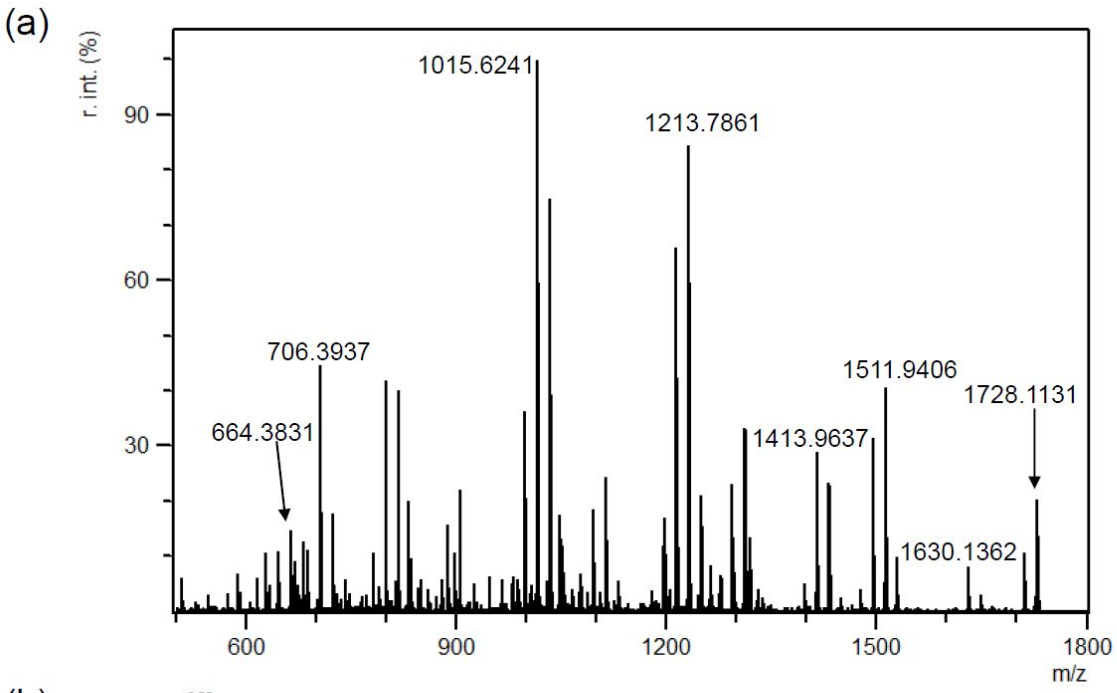

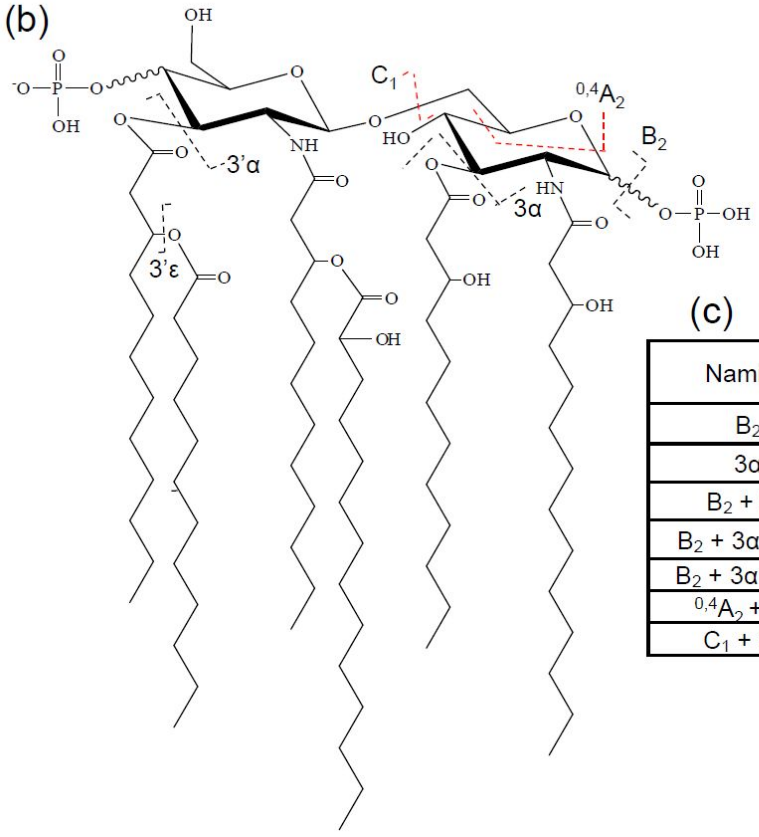

(c)

Naming	*m/z* (theory)	*m/z* (expt)	Error (ppm)
B_2	1630.1362	1630.1148	-13.1
3α	1511.9406	1511.9193	-14.1
B_2 + 3α	1413.9637	1413.9438	-14.1
B_2 + 3α + 3'ε	1213.7861	1213.7701	-13.2
B_2 + 3α + 3'α	1015.6241	1015.6106	-13.3
$^{0,4}A_2$ + 3'α	706.3937	706.3854	-11.7
C_1 + 3'α	664.3831	664.3749	-12.3

Figure S9. (a) FLAT^n mass spectrum from precursor ion at *m/z* 1728.1131 (b) structure of *A. baumannii* expressing *mcr-1* lipid A from FLAT^n, and (c) list of assigned ions.

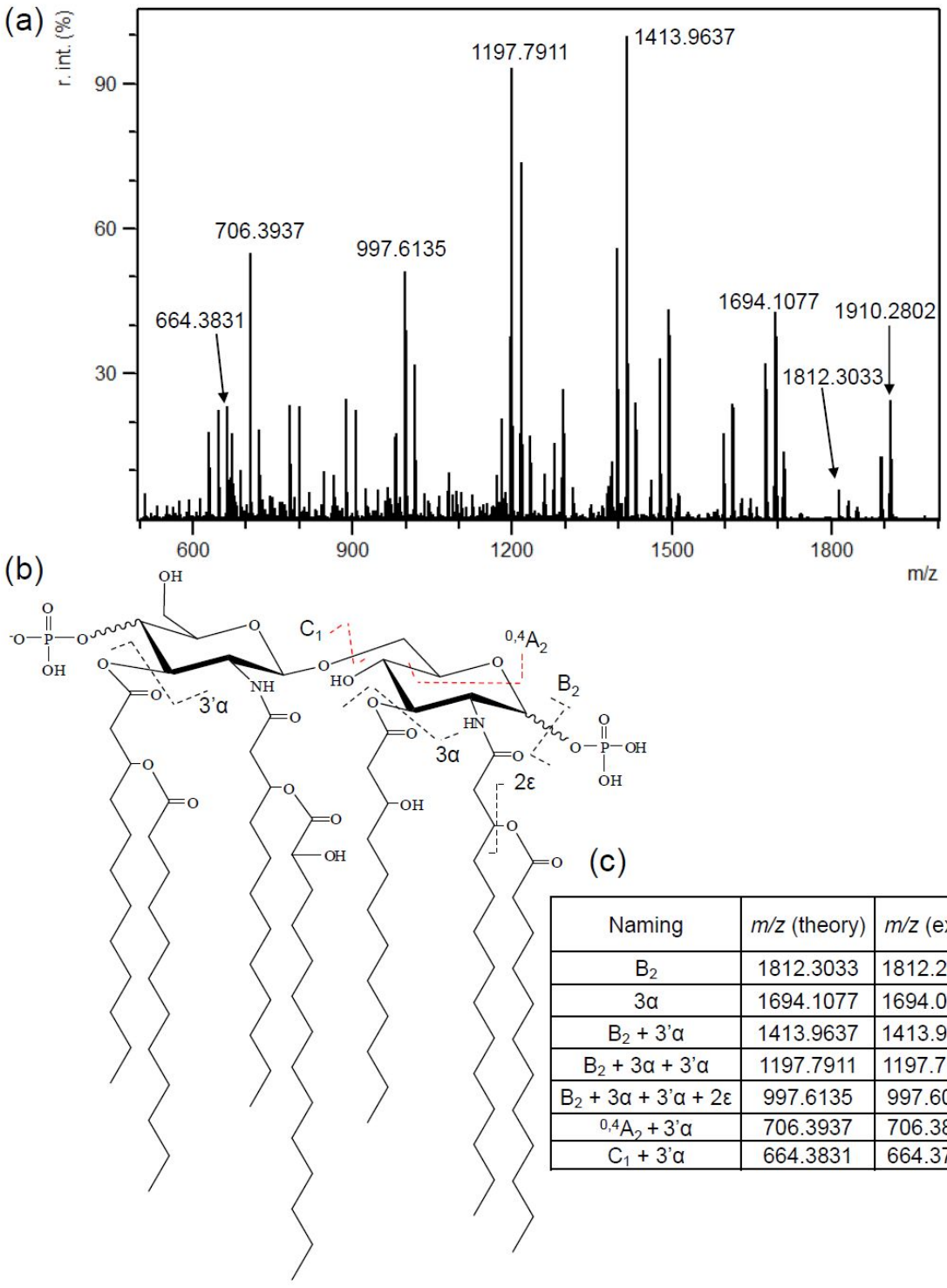

Naming	*m/z* (theory)	*m/z* (expt)	Error (ppm)
B_2	1812.3033	1812.2809	-12.4
3α	1694.1077	1694.0812	-15.6
B_2 + 3'α	1413.9637	1413.9438	-14.1
B_2 + 3α + 3'α	1197.7911	1197.7729	-15.2
B_2 + 3α + 3'α + 2ε	997.6135	997.6005	-13.0
$^{0,4}A_2$ + 3'α	706.3937	706.3859	-11.0
C_1 + 3'α	664.3831	664.3767	-9.6

Figure S10. (a) FLAT^n mass spectrum from precursor ion at *m/z* 1910.2802 (b) structure of *A. baumannii* expressing *mcr-1* lipid A from FLAT^n, and (c) list of assigned ions.

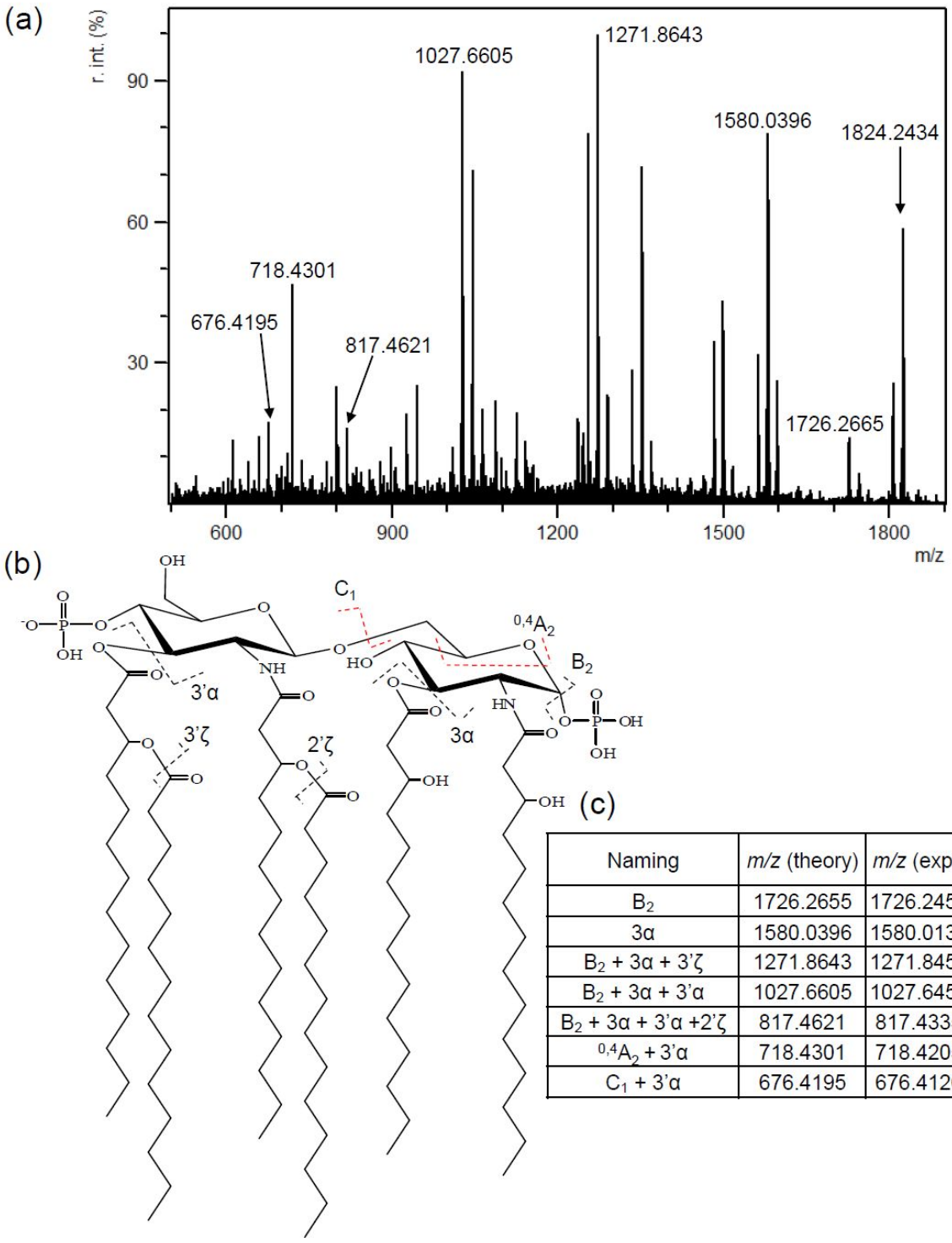

Naming	*m/z* (theory)	*m/z* (expt)	Error (ppm)
B_2	1726.2655	1726.2452	-11.8
3α	1580.0396	1580.0134	-16.6
B_2 + 3α + 3'ζ	1271.8643	1271.8456	-14.7
B_2 + 3α + 3'α	1027.6605	1027.6458	-14.3
B_2 + 3α + 3'α +2'ζ	817.4621	817.4335	-35.0
$^{0,4}A_2$ + 3'α	718.4301	718.4205	-13.4
C_1 + 3'α	676.4195	676.4126	-10.2

Figure S11. (a) FLAT^n mass spectrum from precursor ion at *m/z* 1824.2434 (b) structure of *K. pneumoniae* expressing *mcr-1* lipid A from FLAT^n, and (c) list of assigned ions.

(a)

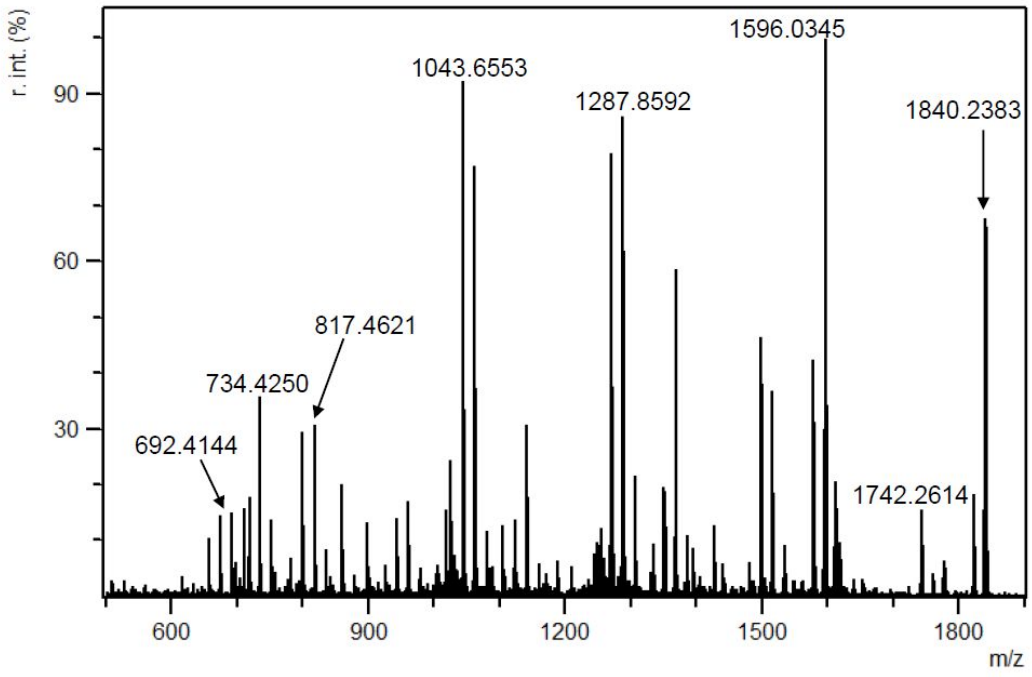

(b)

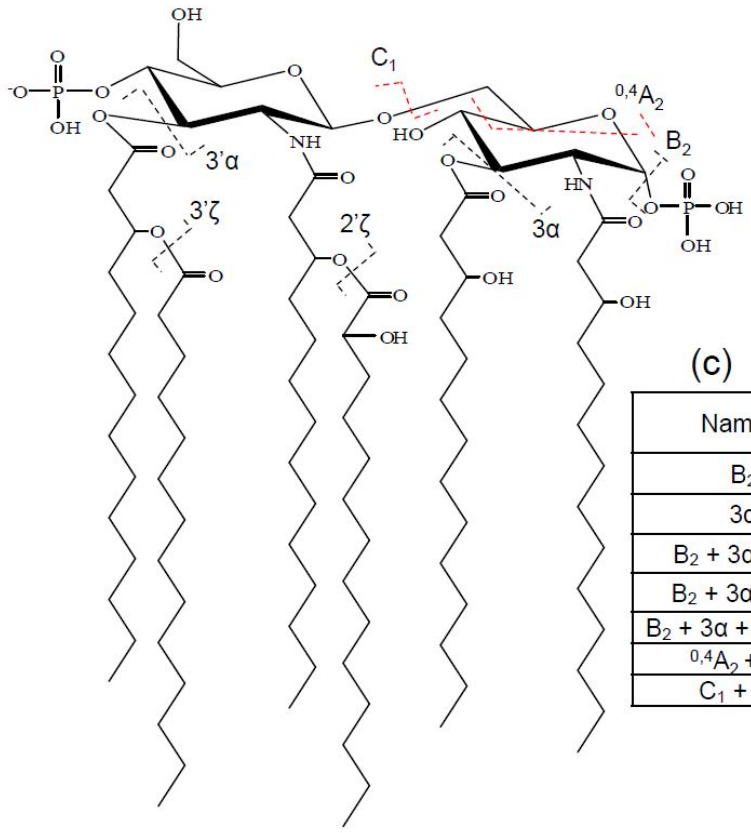

(c)

Naming	*m/z* (theory)	*m/z* (expt)	Error (ppm)
B_2	1742.2614	1742.2356	-14.8
3α	1596.0345	1596.0153	-12.0
B_2 + 3α + 3'ζ	1287.8592	1287.8396	-15.2
B_2 + 3α + 3'α	1043.6553	1043.6413	-13.4
B_2 + 3α + 3'α +2'ζ	817.4621	817.4519	-12.5
$^{0,4}A_2$ + 3'α	734.4250	734.4150	-13.6
C_1 + 3'α	692.4144	692.4040	-15.0

Figure S12. (a) FLAT^n mass spectrum from precursor ion at *m/z* 1840.2383 (b) structure of *K. pneumoniae* expressing *mcr-1* lipid A from FLAT^n, and (c) list of assigned ions.

Table S1. Lists of number of features from two different instruments.

Number of Features			
E. coli		***P. aeruginosa***	
MALDI LTQ-XL-Orbitrap MS	MALDI (timsTOF) MS *	MALDI LTQ-XL-Orbitrap MS	MALDI (timsTOF) MS *
79	244	9	74

*The number of peaks were obtained after de-isotoping process in mMass.

Table S2. Lists of modification site by PEtN.

PEtN phosphate group modification							
Liquid Culture				**Single Colony**			
A. baumannii	*E. coli**	*K. pneumoniae*	*P. aeruginosa*	*A. baumannii*	*E. coli*	*K. pneumoniae*	*P. aeruginosa*
4'	1	4'	4'	4'	4’	4'	4'

*E. coli**: Human urine - 1-phosphate

With Gentamicin - 4’-phosphate

EXPANDED RESULTS & DISCUSSION

Optimization of FLAT^n instrument and single colony experiment

In this experiment, *E. coli* and *P. aeruginosa* were used to examine the fragmentation efficiency. For this part, we employed *E. coli* and *P. aeruginosa* grown in liquid cultures. When MALDI (tims TOF) MS was used, the number of peaks in each mass spectrum was 244 and 74, respectively, after the deisotoping process. On the other hand, the number of peaks from the same sample when we use a MALDI LTQ-XL-Orbitrap MS was 79 and 9 for *E. coli* and *P. aeruginosa*, respectively. This comparison is shown in Table S1. Figure S1A and S1B show the FLAT^n spectra of lipid A of *E. coli* from MALDI (tims TOF) MS and LTQ-XL-Orbitrap MS, respectively. Figure S1C and S1D show the assigned structure of the lipid A and a list of fragments from Figure S1A. The mirror image of FLAT^n mass spectrum clearly indicated that FLAT with MALDI (tims TOF) MS shows higher efficiency of MS^2. For example, MALDI LTQ-XL-Orbitrap MS data in Figure S1B shows handful fragments, such as B_2 and 3α at *m/z* 1698.2352 and 1552.0083, respectively. In contrast, MALDI (tims TOF) MS provides more comprehensive fragments, such as cross-ring fragment with loss of acyl chain, 3'α + $^{0,4}A_2$, at *m/z* 690.3988. Therefore, MALDI (tims TOF) MS was used for all presented FLAT-based bacterial lipid A structural analysis.

Next, in order to determine compatibility of FLAT^n for a single colony experiment, we initially used *E. coli*. A single colony of *E. coli* was picked from the LB agar plate using a pipette tip or a disposable inoculation loop. The single colony on the pipette tip was directly smeared on the ITO slide with both sample preparation method shows similar experimental results, as shown in Figure S2 and 3. Figure S2A shows the image of single *E. coli* single colony selected for analysis. Figure S2B shows FLAT mass spectra obtained from a colony (Top) or inoculation loop (bottom). The *m/z* 1796.21 indicates lipid A ion from *E. coli.* Figure 3S.

Investigation of modification of phosphate in lipid A

Here, we demonstrate the exact location of the phosphate group position modified by the MCR-1 phosphoethanolamine transferase enzyme using FLAT^n in multiple bacterial backgrounds. Figure S5 shows an example of lipid A fragments from *mcr-1 K. pneumoniae* where we identified that the 4'-phosphate group is modified by observation of cross-ring cleavage of lipid A, $^{0,4}A_2$ at *m/z* 1295.8408 (Figure S5A and 5D). The other assigned ions were used to decipher the acyl chain composition and location. Another example of PEtN attachment is *mcr-1 P. aeruginosa* (Figure S6) with the fragmentation pattern assigned as shown in Figure S6B and the characteristic ions are shown in Figure S6D. The fragment ion at *m/z* 913.4961 allowed us to assign the position of PEtN.[6]

Furthermore, we also assigned modification site of phosphate group in lipid A from *mcr-1 A. baumannii*. Figure S7 and 8 show detail structures of modified lipid A. Figure S7 and 8, demonstrates PEtN attachment to hexa-acylated lipid A and hepta-acylated lipid A, respectively, in *mcr-1 A. baumannii*. Specifically, 4'-phosphate group is modified by observation of cross-ring cleavage of lipid A, $^{0,4}A_2$ at *m/z* 1227.7418 in the hexa-acylated lipid A (Figure S7A and 7D). In addition, B_1 ion at *m/z* 1167.7207 provides critical evidence that PEtN was attached to 4'-phosphate group. Hepta-acylated lipid A also shows the same types of fragments as shown in Figure S8A and 8D. Data in all Supplemental Figures were produced from a single colony for each bacterial background.

Determination of structure of diphosphorylated lipid A with acyl chain modification

It has been previously shown that lipid A acyl chain number and length can be altered by environmental factors.[7] For instance, *P. aeruginosa* shows unique acyl chain modifications in isolates obtained from cystic fibrosis patients versus other airway diseases.[8] Therefore, determining acyl chain modification of lipid A can allow us to understand how environmental factors impact lipid A structure. To test if we can use $FLAT^n$ to determine the structure of lipid A with acyl chain modifications, we used *Acinetobacter baumannii* (*A. baumannii*), an opportunistic pathogen in humans.[9] *A. baumannii* was chosen due to the well-documented nature of acyl chain modifications in its lipid A.[3] In *A. baumannii*, hexa-acylated form at *m/z* 1728.1131 (Figure S9) and a hepta-acylated form at *m/z* 1910.2802 (Figure S10) are the major lipid A ions are commonly observed.[10] Since the *m/z* difference of between the two lipid A populations is $\Delta m/z$ 182.17, it is deduced that *m/z* 1910.2802 structure includes a lauric acid addition compared to the *m/z* 1728.1131 structure (C12:0, molecular mass : 200.18, molecular mass of dehydrated form : 182.17). However, it is difficult to identify which acyl chain specifically is modified by lauric acid. By comparing $FLAT^n$ mass spectra, we were able to determine the position of the lauric acid attachment. For instance, the cleavage products of phosphoric acid (B_2) and 3-position acyl chain (3α) from hexa-acylated lipid A correspond with ions *m/z* 1630.1362 and *m/z* 1511.9406, respectively. There are additional ions observed at *m/z* 182.17 ± 0.01 Da at the same neutral loss, such as B_2 and 3α, from hepta-acylated lipid A (*m/z* 1812.3033 and 1694.1077) comparing to hexa-acylated lipid A. Therefore, we can deduce that the lauric acid is not attached at the 3-position acyl chain. In case of the cross-ring cleavage ($^{0,4}A_2$) with acyl chain loss at the 3'α position simultaneously was observed both hexa and hepta-acylated lipid A at *m/z* 706.3937. Moreover, the glycosidic bond cleavage (C_1) with acyl chain loss at the 3'α position was also observed in the hexa and hepta-acylated lipid A at *m/z* 664.3831. Therefore, we can conclude that the lauric acid attached to 2-position of acyl chain. The $FLAT^n$ mass spectra are shown in the Figures S8 and 9.

Another example of acyl chain modification is hydroxylation. Some Gram-negative bacteria produce lipid A with a single hydroxylated secondary acyl chain.[11] For instance, *K. pneumoniae* encodes an oxygen-dependent □-hydroxylase (*lpxO)* gene, which has

been shown previously to be important for survival *in vivo* and resistance to antibiotics.[12] Although identifying the exact site of hydroxylation within the acyl chain is not possible with FLAT^n, it is possible to show which acyl chain is modified with the hydroxyl group. Figure S11 and 12 show examples of how FLAT^n allow us to assign which acyl chain is modified with the hydroxyl group. For instance, the dissociation of B_2 and 3α in Figure 11A produce ions at *m/z* 1726.2655 and 1580.0396, respectively. The same fragments in the hydroxylated-lipid A (Figure S12A) have an addition of 15.99 ± 0.01 from the original *m/z* values (*m/z* 1742.2614 and 1596.0345 shown in Figure S12C). Therefore, we can deduce that the hydroxyl group is not present in the 3-position acyl group. Moreover, the *m/z* value from fragments of the hydroxylated-lipid A have 15.99 additional value from B_2 + 3α + 3'ε or B_2 + 3α + 3'α compared to unmodified lipid A (Figure S11C and 12C). In addition, the cross-ring cleavage with 3'α or glycosidic bond cleavages with 3'α also shows 15.99 ± 0.01 additional values in the hydroxylated-lipid A. Hence, we can deduce that the acyl chain in the non-reducing glucosamine has the additional hydroxyl group. The fragment of B_2 + 3α + 3'α +2'ε shows critical evidence of the secondary acyl chain modified with a hydroxyl group because that fragment has the same value at *m/z* 817.4621 in both unmodified and modified lipid A. From these results, we conclude that the 2'-position acyl chain is modified with the hydroxyl group. This result matches well with literature.[12] These are clear evidence that FLAT^n is a valuable tool to defining acyl chain modification and phosphate modification.

REFERENCES

(1) Yang, H.; Jackson, S. N.; Woods, A. S.; Goodlett, D. R.; Ernst, R. K.; Scott, A. J. *J Am Soc Mass Spectrom* **2020**.
(2) Scott, A. J.; Flinders, B.; Cappell, J.; Liang, T.; Pelc, R. S.; Tran, B.; Kilgour, D. P.; Heeren, R. M.; Goodlett, D. R.; Ernst, R. K. *Pathog Dis* **2016**, *74*.
(3) Liu, Y. Y.; Chandler, C. E.; Leung, L. M.; McElheny, C. L.; Mettus, R. T.; Shanks, R. M. Q.; Liu, J. H.; Goodlett, D. R.; Ernst, R. K.; Doi, Y. *Antimicrob Agents Chemother* **2017**, *61*.
(4) Yang, H.; Jackson, S. N.; Woods, A. S.; Goodlett, D. R.; Ernst, R. K.; Scott, A. J. *J Am Soc Mass Spectrom* **2020**, *31*, 2495-2502.
(5) Niedermeyer, T. H.; Strohalm, M. *PLoS One* **2012**, *7*, e44913.
(6) Nowicki, E. M.; O'Brien, J. P.; Brodbelt, J. S.; Trent, M. S. *Mol Microbiol* **2015**, *97*, 166-178.
(7) Steimle, A.; Autenrieth, I. B.; Frick, J. S. *Int J Med Microbiol* **2016**, *306*, 290-301.
(8) Ernst, R. K.; Yi, E. C.; Guo, L.; Lim, K. B.; Burns, J. L.; Hackett, M.; Miller, S. I. *Science* **1999**, *286*, 1561-1565.
(9) Howard, A.; O'Donoghue, M.; Feeney, A.; Sleator, R. D. *Virulence* **2012**, *3*, 243-250.
(10) Dortet, L.; Potron, A.; Bonnin, R. A.; Plesiat, P.; Naas, T.; Filloux, A.; Larrouy-Maumus, G. *Sci Rep* **2018**, *8*, 16910.
(11) Lo Sciuto, A.; Cervoni, M.; Stefanelli, R.; Spinnato, M. C.; Di Giamberardino, A.; Mancone, C.; Imperi, F. *Pathogens* **2019**, *8*.
(12) Llobet, E.; Martinez-Moliner, V.; Moranta, D.; Dahlstrom, K. M.; Regueiro, V.; Tomas, A.; Cano, V.; Perez-Gutierrez, C.; Frank, C. G.; Fernandez-Carrasco, H.; Insua, J. L.; Salminen, T. A.; Garmendia, J.; Bengoechea, J. A. *Proc Natl Acad Sci U S A* **2015**, *112*, E6369-6378.